IEEE
THE INSTITUTE OF ELECTRICAL AND ELECTRONICS ENGINEERS INC.

SIGNAL PROCESSING
ALGORITHMS, ARCHITECTURES, ARRANGEMENTS, AND APPLICATIONS
SPA 2015
September 23-25th, 2015, Poznań, POLAND

Segmentation of 3D magnetic resonance brain vessel images based on level set approaches

Tomasz Woźniak
Lodz University of Technology
Institute of Electronics
Lodz 90-924, Poland
Email: tomasz.wozniak11@gmail.com

Michał Strzelecki
Lodz University of Technology
Institute of Electronics
Lodz 90-924, Poland
Email: michal.strzelecki@p.lodz.pl

***Abstract*—Quantitative modeling of brain vasculature is important for diagnosis of vessel pathologies as well as for surgery treatment planning. Magnetic resonance angiography (MRA) provides reliable visualization of vessel tree structure and its organization. Accuracy of vessel segmentation from MRA is an important step in model building; its accuracy influences obtained model quality. This paper presents three level set based segmentation approaches, including one that represents original authors contribution. These methods are combined together with vesselness function estimated for analyzed images. Presented algorithms were applied both for artificial and real brain 3D MR images. Analysis results along with discussion are also included.**

I. INTRODUCTION

Extraction of the vascular network from magnetic resonance image is very significant in diagnosis and therapy of circulatory system. Analysis of MRA images provides a quantitative description of vessels architecture. Furthermore, the obtained model of vessels allows diagnosing lesions of vascular network, such as stenosis.

A number of imaging modalities are implemented for angiographic images acquisition. Basic approach is based on radio-opaque contrast agent and X-rays used for imaging. However, the method is invasive and nowadays may be displaced by MR imaging with the help of specific angiographic sequences e.g. time of flight (ToF). Modern scanners (with 3T magnetic field) approaches in image resolution to the X-ray based computer tomography. As a result, obtained images enables visualization of small-diameter blood vessels (<1 mm). Thus, high quality quantitative models can be build based on extracted vasculature.

There are several methods used for segmentation of brain blood vessels. They can be divided into 3 groups. First one comprises methods of image processing, e.g. scale-space or mathematical morphology filtering, finding skeleton of blood vessel structure [1], [2], [3]. Another group uses mathematical modeling of the image, e.g. through fitting parameterized hypersurfaces to the shape of veins or arteries. These methods use active contours or level sets [4], [5], [6], [7]. The third group is based on a priori knowledge about the blood vessel system, collected in anatomical atlases [8]. Such atlases serve as certain reference patterns used for presentation and evaluation of the results of segmentation of the vessels obtained for diverse individuals. Reviews of the methods of blood vessel image segmentation can be found in literature [9]. Despite of much effort in the field of MRA image analysis, the problem of precise segmentation of the vascular network from MRA is still unsolved. On the other hand the segmentation is a crucial step since its accuracy directly influences the quality of vasculature model obtained in further analysis. Quantitative description of the model will provide information on vessel tree geometry like e.g. diameter of individual vessels and their volume.

The interest in level set based segmentation algorithms has grown recently, as a result of relative high speed of these algorithms execution and the method ability of accurate modeling of complex shapes of the blood vessels. These methods are often used as one of the stages of the segmentation procedure [10], [11]. This work is aimed at comparison and development of a number level set based segmentation method. We also focus on some preprocessing techniques applied to the image before the segmentation takes place. Moreover, the article describes our own extension of the LS approach. As a level set function we implement Chan-Vese mathematical model [12], widely used for blood vessel extraction. Prior to the segmentation, two preprocessing patches are applied: Hessian filtration [7] and estimation of gradient vector flow (GVF) [13]. The latter is used to emphasize image gradients thus making vessel extraction more efficient.Next, for preprocessed image vesselness function (VF) [6] is estimated. It emphasizes tubular structures in the image making vessel extraction more reliable by following segmentation algorithms. Finally, the LS segmentation is performed. Flowchart of image analysis is presented in Fig. 1. LS1 means segmentation based on classic Chan-Vese level set model only. LS2 corresponds to solution proposed by Forkert [14]. It considers additional energy term added to LS functional to ensure more accurate vessel extraction. LS3 indicates our proposal, that extends Forkert approach to muliscale analysis.

II. MATERIALS AND METHODS

A. Analyzed images

To evaluate performance of candidate image segmentation techniques, from qualitative as well as quantitative points of view, more realistic numerical phantoms were designed. To

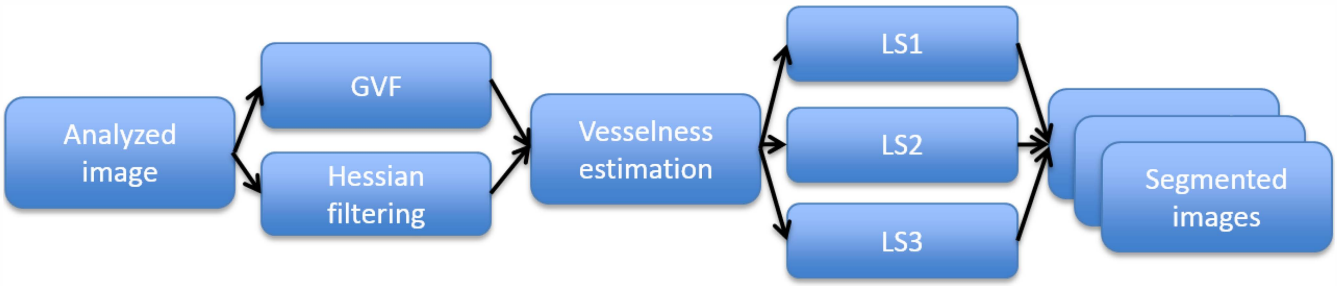

Fig. 1: Block diagram of image analysis steps

Fig. 2: MIP of original MR brain image

Fig. 3: MIP of the brain image after contrast nonuniformity correction

model real-world vessel trees, cylinders of different diameters were connected together. To generate such vascular tree images, the computer simulator of tree growth was developed and implemented [15]. The tree consists of 4000 outlet branches and each tree image had a size of 256x256x256 voxels. Tree image was corrupted by the Gaussian noise with zero mean and standard deviation $\sigma^2 = 6$.

Volunteer brain data were acquired by using the TOF-SWI sequence in Friedrich Schiller University in Jena, Germany. Signal intensity changes occur along the slice encoding direction due to merging of the slabs and by e.g., applying of a ramped rf-pulse (TONE pulse). Furthermore, signal inhomogeneities are introduced by data acquisition with multiple receiving MR coils and combining of the different MR channels using the sum of squares reconstruction. These effects are shown in Fig. 2; if not handled, they can deteriorate the quality of further processing [16]. To remove signal intensity artifact the histogram equalization-based procedure was applied [17]. Corrected image is shown in Fig. 3.

B. Vesselness function (VF)

The purpose of vesselness function is to enhance vessel structures with eventual goal of vessel segmentation [7].The vessel enhancement is a filtering process that searches tubular structures in image. The detection of vessel is based on analysis of second order information (Hessian) obtained by image convolution with second order Gaussian derivatives. The scale in this filtration is established by parameter s in Gaussian derivative equation. Hessian matrix is calculated for every voxel in the three dimensional image. Comparison of eigenvalues of this Hessian matrix to certain values is used for detection of tubular structure. The vesselness function equation for one scale s is presented in [6]. Calculating the VF for many scales and selecting the maximum value for each scale enables emphasizing of vessel branches with different diameters [6].

C. Gradient vector flow (GVF)

This approach was proposed in [13] to solve problems associated with initialization and poor convergence of active contour algorithms. GVF is an external force computed as a diffusion of the gradient vectors of a gray-level or binary edge map derived from the image. The GVF is defined as the vector field V(x) that minimizes:

$$E(V) = \iiint \mu|\nabla V(x)|^2 + |\nabla I(x)|^2|V(x) - I(x)|^2 dx \quad (1)$$

where x represent voxel coordinates, and μ is a regularization parameter adapted according to the amount of image noise.

The GVF results in image smoothing where the initial vector magnitudes are small, while keeping vectors with high magnitude nearly equal. In practice, the GVF preserves even weak structures while being robust to large amounts of noise [8]. In [18] GVF approach was proposed for detecting of tubular objects (including blood vessels) without the need for a multi-scale analysis (by means of Hessian filtering). Reported advantage when compared to multiscale filtering was more precise detection of thin structures laying close each other avoiding diffusion of nearby structures into one another. The GVF was combined together with Frangi vesselenss function and applied both to artificial as well as to CT angio images providing accurate segmentation results [18].

D. Chan-Vese Level-Set method

Level-set method based on Chan-Vese mathematical model is versatile and widely used in biomedical image segmentation. The main idea in level set active contour model is to iteratively evolve a curve that is controlled by some parameters estimated from the image. The motion of the curve is obtained by solving the curve evolution partial differential equation (PDE) [12], adapted to three-dimensional data space. Finally, the curve ends its evolution by fitting to objects boundaries within the given image. This method is an energy minimalization based segmentation. The two dimenstional PDE is presented in Chan and Vese paper [12].

E. Improved LS model

In this method proposed by Forkert in [14] a vesselness function is estimated, which quantifies the likeliness of each voxel to belong to a bright tubular-shaped structure as, described in subsection B. Level set model is extended by applying the weights of the internal energy, which are locally adapted based on the vesselness function information. The main idea of Forkert approach is to bias the internal depending on differences between directions of level set function expansion and the main eigenvector extracted from vesselness function. This eigenvector point at local vessel directionality. When the angle between eigenvector and level set gradient is small, then this term is high encouraging further LS hipersurface evolution. Otherwise, it blocks LS expansion outside the vessel, as shown in Fig. 2. Moreover, there is also anoter term representing a vesselness force added to level set equation. This additional energy term is used to actively drive the contour along the vessels. In this paper we adapted the equations presented in [14] to the Chan-Vese level set algorithm.

$$F(\phi) = E_e(\phi) + E_i(\phi, \omega^\phi) + \nu(\phi) \tag{2}$$

Where $E_e(\phi)$ and internal energy $E_i(\phi, \omega^\phi)$ with vesselness dependent weight. Third term $\nu(\phi)$ is the vesselness force. The external energy equation does not change and it is the same as equation presented in [12]. However, the internal energy implements the additional weight ω^ϕ. Extended internal energy equation used in this method is presented below.

$$E_i(\phi, \omega^\phi) = \int_\omega ||\omega^\phi \nabla H(\phi(x))|| dx \tag{3}$$

The ω^ϕ in this equation is used to adapt the weight of the internal energy depending on the angle α between eigenvector e_1, which is the first eigenvector obtained from Hessian and $\nabla\phi$. The ω^ϕ is obtained by:

$$\omega^\phi(x) = \mu \cdot (1 - \cos(\alpha(x))) \tag{4}$$

where the cosine is estimated by:

$$\cos(\alpha(x)) = \frac{e_1 \cdot \nabla\phi}{||e_1|| \cdot ||\nabla\phi||} \tag{5}$$

The scaling parameter μ is defined in [12] as curve length. If one needs detection of as many objects as possible with different sizes, then μ should be small. If larger objects should be detected only (for example objects formed by grouping), then larger μ should be selected. According to that, when the cosine in (4) is close to 1 (eigenvector and gradient are parallel) ω^ϕ parameter will be close to 0. Otherwise, it will be equal to the preset value.
The energy functional $\nu(\phi)$, which includes a vesselness force term is defined as:

$$\nu(\phi) = \omega^V \int_\omega H(\phi(x)) cos(\alpha(x)) \sqrt{V(x)} dx \tag{6}$$

The weight of this term is highest in case α is close to 0°or 180°and for large vesselness values forcing a level set evolution towards tubular structures [14].

F. Proposed modification

Method proposed by Forkert is very useful for segmentation of network, which consist of vessels with similar radii. However, the real vasculature contains vessels with different diameters. Thus multiscale approach is needed to correctly emphasize vessels with different size in the vesselness function. Thus, VF should be calculated for multiple Hessian filters with different sigma. Selection of number of implemented filters and their corresponding sigma values depend on vessel radii variation in the analyzed image. Moreover, the multiscale effect should be also reflected in weight estimation (4). This means that eigenvector e_1 that corresponds to the largest eigenvalue of hessian matrix should be also estimated for each of considered scales s. Then, the vesselness function equation will be modified as follows.

$$V_{max}(x) = \max_{s_{min} < s < s_{max}} (V(x, s)) \tag{7}$$

The $V_{max}(x)$ The Vmax(x) value is calculated for every voxel in the image and further used for estimation of the vesselness force in equation (5). Furthermore, this value is used to establish the eigenvector e_1 for calculation of $\cos(\alpha(x))$. The e_1 are evaluated for every filtration scale. For calculation of internal energy weight, the e_1 vector corresponding to the $V_{max}(x)$ value is used. The e_1 estimated for optimal scale should be parallel with $\nabla\phi$ inside the vessel and almost perpendicular outside. Proposed solution should adjust the ω^ϕ weight appropriately. Combining this with modified vesselness function (estimated for multiscale filtering thus taking maximum values for every image voxel according to

the optimal scale) should lead to improved segmentation when compared to approach suggested in [14]. Presented method was implemented in C♯ programming language as Windows application.

III. Results

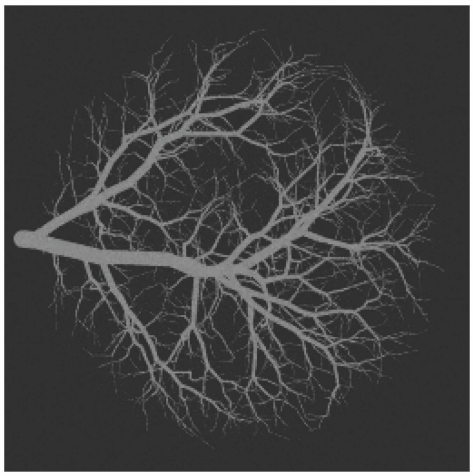

Fig. 4: MIP of distorted artificial tree image

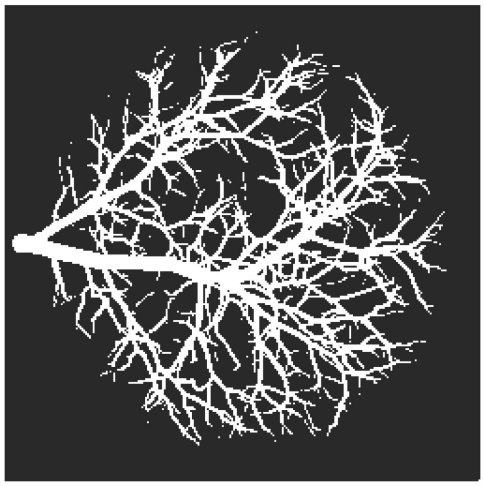

Fig. 5: Result of HF + VF + LS1

Artificial tree image was analyzed according to diagram shown in Fig. 1. Its maximum intensity projection is shown in Fig. 4. Next, Hessian filtering (HF) for scales 0.4 and 0.8 was performed. Independently, GVF were also evaluated. For both preprocessing results VF was estimated. Obtained images were fed into 3 versions of LS approach: original Chan-Vese model (LS1), Forkert modification (LS2), and finally, our approach (multiscale version of Forkert approach, LS3). MIPs of segmentation results obtained for these methods are shown in Figs. 5-8. After segmenting the image processed by GVF with LS1 technique it was found that in this case thick branches are not processed correctly (only vessel walls are detected leaving empty space inside). This is explained by properties of GVF operator that emphasizes image gradients

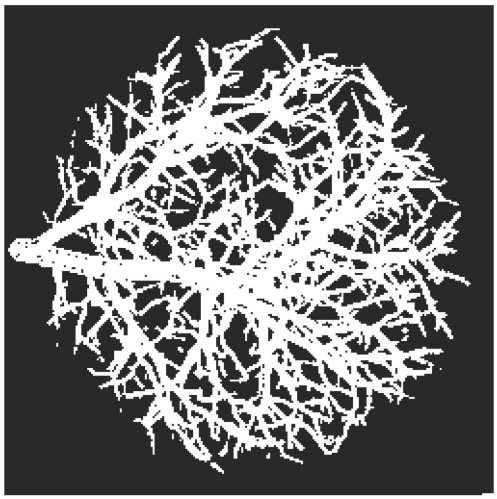

Fig. 6: Result of GVF + VF + LS1

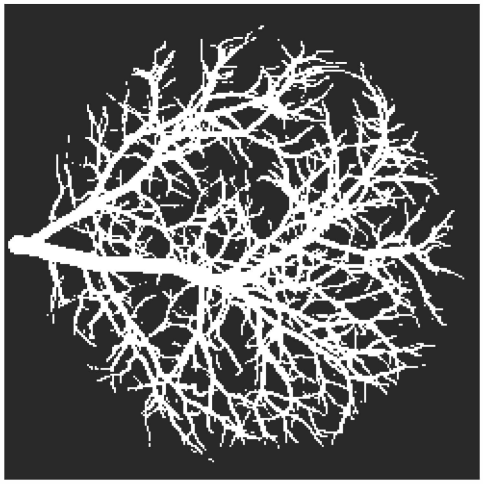

Fig. 7: Result of HF + VF + LS2

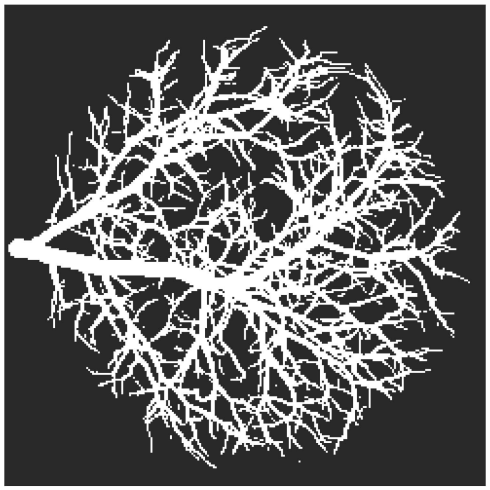

Fig. 8: Result of HF + VF + LS3

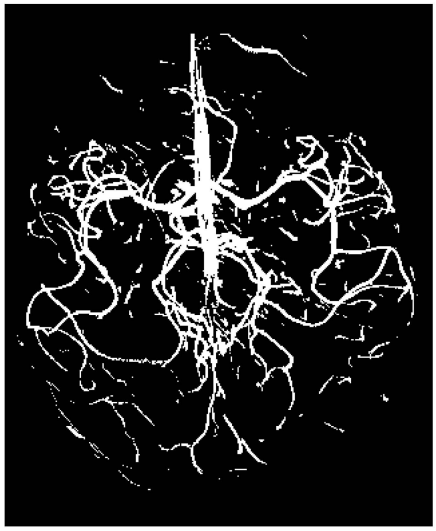

Fig. 9: Result of HF + VF + LS1

and reduces areas with slowly varying brightness (like internal vessel part). Since this effect leads to imprecise detection of thick vessels, LS2 and LS3 techniques were not applied for GVF image. For quantitative evaluation of segmentation results, the Jaccard coefficient was estimated. It expresses the similarity between segmented image and binarized version of undistorted tree phantom. Its value varies from 0 to 1 where the highest one represents the perfect segmentation. J values are given in Table 1.

TABLE I: Estimated J coefficients for different preprocesss-ing/segmentation methods

Method	Jaccard
HF + VF + LS1 (Fig. 5)	0.43
GVF + VF + LS1 (Fig. 6)	0.52
HF + VF + LS2 (Fig. 7)	0.58
HF + VF + LS3 (Fig. 8)	0.64

Second test was performed on MR ToF image after contrast artifact correction. The same preprocessing was applied as in the case of tree image (VF estimation followed by Hessian filtering and GVF evaluation). Then LS1, LS2 and LS3 segmentation approaches were used. For the same reason, LS2 and LS3 were not applied to the GVF processed brain images. Analysis results are presented in Figs. 9-12.

IV. Discussion and conclusion

Results obtained for tree image shows that there is continuity of detected blood vessels in most cases. The only exception is LS1 where a number of thin vessels are not connected each other. Also, in all cases the noise does not distorted obtained vessel structure. LS2 outperforms LS1 providing more accurate detection of thin vessels. It can be explained by additional energy term added to the LS model. This energy, represented by vesselness function helps the level set curve in better fitting

Fig. 10: Result of GVF + VF + LS1

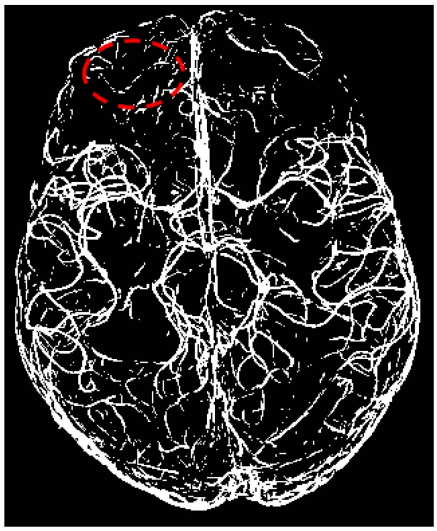

Fig. 11: Result of HF + VF + LS2

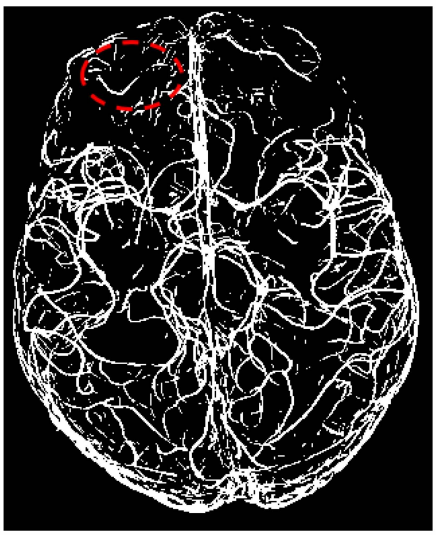

Fig. 12: Result of HF + VF + LS3

to the original vessel shape. For similar reason, LS3 provides even better result by considering multiscale vessleness function. It provides more accurate vessel representation when analyzed tree branches differ in their diameter. The price paid for emphasizing of thin vessels by vesselness function is vessel thickening; this is especially visible for GVF-processed image. Described effects are reflected in J values (Table 1) obtained for different segmentation approaches, indicating LS3 as a most accurate one.

Evaluation of brain image segmentation can be done by visual assessment only. However, partially similar effects can be observed as in the case of tree images segmentation. LS1 results in good detection of thick vessels, however a number of thin ones are omitted. Also, the continuity of some fragments of vessel network is lost. Application of LS2 significantly increases amount of thin vessels detected, however on the same time artifacts appear. This is emphasized by LS3: increased number of thin branches when compared to LS2, but also a presence of a number of artifacts in resulting image. Advantage of LS3 over LS2 lays also is in more continuous network, see marked fragment in Fig. 11 and 12. The GVF-based result shows a big disadvantage of this method - it detects a lot of artifacts as a result of image gradient enhancement (in ToF images, beside the vessels, other tissues are also partially visible).These artifacts are further removed by VF but, unfortunately, together with vessels with small diameters. Thus fragments of thick vessels are detected only, along with artifacts of larger size.

For both artificial tree image and MR brain image Forkert modification outperforms classic LS approach. However, segmentation accuracy strongly depends on filter scale. Its high value can cause thickening of vessels with small diameter. On the other side, selection of to small scale does not detect vessel inner part, especially when branch diameter is large. This problem is partially solved by our approach. Introduction of energy term to the LS model that considers multiscale vesselness function enables correct detection of branches with different diameters. This leads to better characterization of segmented vasculature resulting in more precise brain vessel geometric model.

To further improve detection of blood vessels, there is a need to eliminate of artifacts that distort segmentation results. Another problem to be solved is continuity monitoring of detected vessels. Analysis results should be verified on digital vessels phantoms obtained by means of simulated MR angiography [19]. Preliminary segmentation results were considered by radiologist as promising, however further examination is much needed. All above issues will be topics of further research.

ACKNOWLEDGMENT

The Authors would like to thank Prof. Juergen Reichenbach from Friedrich Schiller University in Jena, Germany for delivering brain MR images and Dr Marek Kociński from the Institute of Electronics, LUT for providing artificial tree phantoms.

The project has been funded by National Science Centre, Poland (decision No. DEC-2013/08/M/ST7/00943).

REFERENCES

[1] E. Bullitt, D. A. Reardon, J. K. Smith, A review of micro- and macrovascular analyses in the assessment of tumor-associated vasculature as visualized by MR, Neuroimage, 37, 2007, s. 116-119.

[2] C. Kirbas, F. Quek, A Review of Vessel Extraction Techniques and Algorithms, ACM Computing Surveys, 36(2), 2004, s. 81-121

[3] J. Suri, K. Liu, L. Reden, S. Laxminarayan, A Review on MR Vascular Image Processing Algorithms: Acquisition and Prefiltering: Part I and II, IEEE Transactions on Information Technology In Biomedicine, 6(4), 2002, s. 324-337 i 338-360

[4] R. Manniesing, B.K. Velthuis, M.S. van Leeuwen, I.C. van der Schaaf, P.J. van Laar, W.J. Niessen, Level set based cerebral vasculature segmentation and diameter quantification in CT angiography, Medical Image Analysis, 10, 2006, s. 200-214

[5] M. Strzelecki, A. Materka, M. Kociński, P. Szczypiński, A. Deistung, J. Reichenbach, Ocena metody zbiorów poziomicowych w zastosowaniu do segmentacji trójwymiarowych obrazów fantomów cyfrowych oraz obrazów naczyń krwionośnych mózgu ToF-SWI rezonansu magnetycznego, Inżynieria Biomedyczna (Acta Bio-Optica et Informatica Medica), 16, 2, 2010, s. 167-172

[6] F. Frangi, W. J. Niessen, K. L. Vincken, M. A. Viergever, Muliscale Vessel Enhancement Filtering, Proc. of MICCAI 1998, 1998, s. 130-137

[7] Y. Sato, S. Nakajima, H. Atsumi, T. Koller, G. Gerig, S.Yoshida, R. Kikinis, 3D Multi-Scale Line Filter for Segmentation and Visualization of Curvilinear Structures in Medical Image, 1997, http://www.spl.harvard.edu/archive/splpre2007/pages/papers/yoshi/cr.html

[8] M. A. Bernstein, J. Huston, C. Lin, G. F. Gibbs, J. P. Felmlee, High-resolution intracranial and cervical MRA at 3.0T: technical considerations and initial experience, Magn Reson Med, 46(5), 2001, s. 955-962

[9] N. Passat, C. Ronse, J. Baruthio, J.-P. Armspach, Automatic parameterization of grey-level hit-or-miss operators for brain vessel segmentation, Proc. of ICASSP 2005, 2, s. 737-740

[10] J. R. Reichenbach, E. M. Haacke, High Resolution BOLD Venographic Imaging: A Window into Brain Function, NMR Biomed, 14(7-8), 2001, s. 453-467

[11] M. Strzelecki, P. Szczypiński, A. Materka, M. Kociński, A. Sankowski, Level-set segmentation of noisy 3D images of numerically simulated blood vessels and vascular trees, Proceedings of 6th International Symposium on Image and Signal Processing and Analysis, 16-18 September 2009, Salzburg, Austria, pp. 742-747

[12] T. F. Chan, L. A. Vese, Active Contours Without Edges. IEEE Transaction on Image Processing, 10(2), 2001, pp. 266-277

[13] Xu, C., Prince, J.L.: Snakes, shapes, and gradient vector flow. IEEE Transactions on Image Processing 7(3), 359369 (1998)

[14] Forkert, N.D., Schmidt-Richberg, A., Fiehler, J., Illies, T., Möller, D., Säring, D., Handels, H., Ehrhardt, J.: 3D cerebrovascular segmentation combining fuzzy vessel enhancement and level-sets with anisotropic energy weights. Magnetic Resonance Imaging 31, 2013, pp. 262-271

[15] M. Kociński, A. Klepaczko, A. Materka, M. Chekenya, A. Lundervold, 3D image texture analysis of simulated and real-world vascular trees, Computer Methods and Programs in Biomedicine, 107(2), 2012, pp. 140-154

[16] A. Materka, M. Strzelecki, On the Importance of MRI Nonuniformity Correction for Texture Analysis, Proc. of IEEE SPA 2013, 26-28 September 2013, Poznań, Poland, pp. 118-123

[17] Kholmovski EG, Alexander AL, Parker DL. Correction of slab boundary artifact using histogram matching. J Magn Reson Imaging 2002;15(5):6107

[18] C. Bauer, H. Bischof, A Novel Approach for Detection of Tubular Objects and Its Application to Medical Image, Proc. of DAGM 2008, LNCS 5096, pp. 163-172

[19] A. Klepaczko, P. Szczypiski, G. Dwojakowski, M. Strzelecki, A. Materka, Computer simulation of magnetic resonance angiography imaging: Model description and validation, PLoS ONE, 9(4), 2014, DOI: 10.1371/journal.pone.0093689